

Probing the Intrinsic Switching Kinetics of Ultrathin Thermoresponsive Polymer Brushes**

Crispin Amiri Naini, Steffen Franzka, Sven Frost, Mathias Ulbricht, and Nils Hartmann*

Stimuli-responsive polymers have become versatile materials for the design and fabrication of smart functional devices, such as adaptive microoptics, microfluidic chips, membranes, and sensors.^[1] Controlled reaction schemes allow the build-up of surface-grafted polymer brush films with thicknesses down to the sub-100 nm range.^[2] This approach opens up an avenue towards miniaturized device structures with unprecedented functionalities.^[3] To establish design rules and estimate device performance, a detailed fundamental knowledge of the switching kinetics of such ultrathin polymer films is of utmost importance.^[3,4] It is worth noting that despite the ultrathin nature of these films, most previous studies revealed fairly long response times of several seconds or more.^[4] High-speed measurements, though, are challenging in many respects and hence data on the intrinsic switching kinetics still are largely missing.^[3,4] Herein we show a novel stroboscopic photothermal laser manipulation technique that allows for real-time measurements of the intrinsic temperature-dependent switching kinetics of poly(*N*-isopropylacrylamide) (PNiPAAm) brushes at the water/substrate interface.

PNiPAAm is a classic thermoresponsive polymer that exhibits a lower critical solution temperature (LCST) in water. Below 32 °C the polymer is swollen, whereas the material dehydrates and collapses above this temperature. In their pioneering studies on macroscopic PNiPAAm gels,

Tanaka and co-workers related the response time τ to the diffusion coefficient D of the polymer network and the size d of the gel: $\tau = d^2/D$.^[5] Because of the diffusion-limited process, response times of polymer gels and films with dimensions in the micro- and millimeter range are on a second to hours time scale.^[5,6] Much shorter response times generally are expected for ultrathin polymer films. Considering sub-100 nm films, an estimate with $D = 3 \times 10^{-7} \text{ cm}^2 \text{ s}^{-1}$ from reference [5a] gives values in the milli- or microsecond range. Thus, the investigation of the intrinsic switching kinetics of such coatings requires excellent temporal resolution of the experimental technique applied. In addition to fast detection methods, rapid heating techniques are essential in order to instantly establish a constant stimulus. Conventional techniques clearly are limited in this respect. Further requirements arise because of the soft and sensitive nature of the polymeric layer and the necessity to probe structural changes at a hidden interface. Overall, these constraints impeded the investigation of the intrinsic switching kinetics of ultrathin PNiPAAm brushes till date. In a recent study, a response time of several seconds has been reported, which may be considered as an upper limit.^[4d]

To cope with the aforementioned challenges, we set up an all-optical micromanipulation/-characterization technique (Figure 1a). Taking advantage of our experience in photothermal laser processing,^[7] a microfocused continuous wave (cw) laser beam ($\lambda = 532 \text{ nm}$, $d_{1/e^2} = 5 \mu\text{m}$) is used for rapid heating of the water/substrate interface.^[8] Surface-oxidized Si/Ti-coated glass plates were chosen as substrates. A surface-grafted PNiPAAm brush layer is grown on top of the coated glass plates by atom transfer radical polymerization following standard procedures.^[9] The particular design of the substrates serves two functions. Firstly, the glass plates allow for convenient back surface laser heating of the multilayered coating. Secondly, interference effects at the water/polymer/substrate-interface provide the basis for noninvasive, label-free video monitoring of the photothermally induced switching of the polymeric coating by using an ordinary reflective optical microscope with water immersion optics and a charge-coupled device (CCD) camera.

Because of the microscopic size of the heated area, the temperature of both sample and water essentially remains unchanged even after prolonged measurements over several hours.^[8a] During laser irradiation, a stationary temperature profile is established on a microsecond timescale.^[7] Once the laser is switched off, the heated surface area rapidly cools to room temperature.^[7,8a] This procedure allows for stroboscopic measurements by periodic photothermal laser manipulation (Figure 1b). The temporal resolution in this operation mode is determined by the shutter time of the camera, which is set to 0.1 ms.

[*] C. Amiri Naini, Dr. S. Franzka, Priv.-Doz. Dr. N. Hartmann
CeNIDE—Center for Nanointegration Duisburg-Essen
47057 Duisburg (Germany)
and
Fakultät für Chemie, Physikalische Chemie
Universität Duisburg-Essen, 45117 Essen (Germany)
Fax: (+49) 201-183-3228
E-mail: nils.hartmann@uni-due.de

S. Frost, Prof. Dr. M. Ulbricht
CeNIDE—Center for Nanointegration Duisburg-Essen
47057 Duisburg (Germany)
and
Fakultät für Chemie, Technische Chemie II
Universität Duisburg-Essen, 45117 Essen (Germany)

[**] Financial support by the Deutsche Forschungsgemeinschaft (DFG, Grant HA-2769/3-1), the BASF Coatings AG, the European Union, and the Ministry of Innovation, Science and Research of the State of North Rhine-Westphalia in Germany (NanoEnergieTechnikZentrum, NETZ, Objective 2 Programme: European Regional Development Fund, ERDF) is gratefully acknowledged. We are grateful to Martin Jerman from the optical shop at the University of Duisburg-Essen for the preparation of the Si/Ti/glass samples and help with the thin film optical calculations. N.H. also gratefully thanks Eckart Hasselbrink for his continuing support.

Supporting information for this article is available on the WWW under <http://dx.doi.org/10.1002/anie.201100140>.

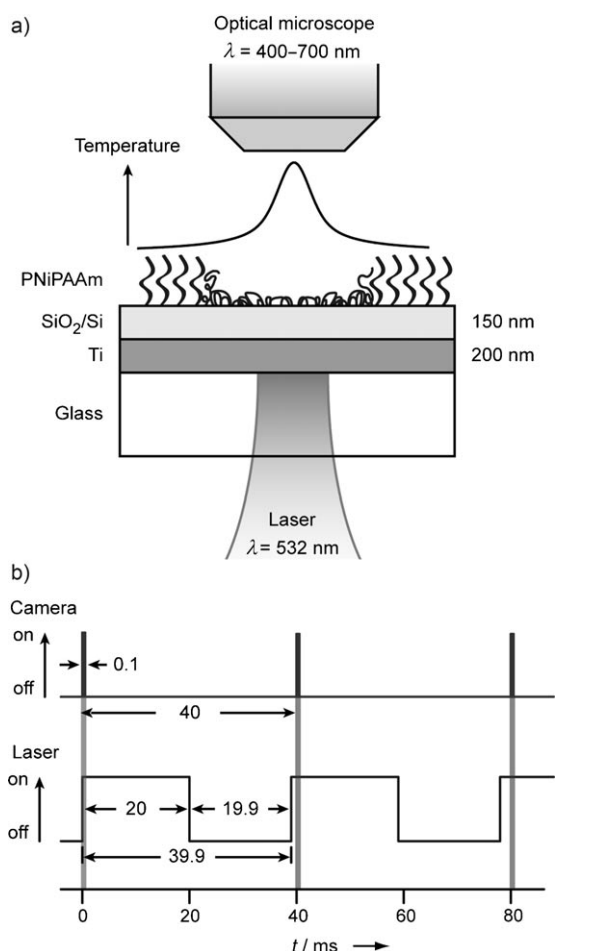


Figure 1. a) Schematic of the micromanipulation/-characterization principle showing, from bottom to top, the focused laser beam for photothermal manipulation, the multilayered sample with the PNiPAAm brush layer on top, the surface temperature profile at the water/polymer interface during laser irradiation, and the water immersion objective of the optical microscope for characterization. b) Stroboscopic effect exploited in the kinetic measurements. The CCD camera is operated at a frame rate of 25 fps equivalent to an acquisition period of 40 ms; the shutter time is set to 0.1 ms. Periodic laser manipulation is carried out at a period of 39.9 ms with on and off times set to 20 ms and 19.9 ms, respectively. As depicted, at these settings, in each frame a distinct time interval during laser heating and cooling is captured. A complete sequence of consecutive snapshots is acquired in 15.96 s, which is equivalent to an apparent slow motion factor of 400.

All following experiments are carried out with PNiPAAm brush layers with a collapsed film thickness of 65 nm at a grafting density of approximately $5 \times 10^{13} \text{ cm}^{-2}$.^[9] Figure 2a shows an optical micrograph of such an ultrathin PNiPAAm film upon back surface laser irradiation at long times equivalent to cw exposure. Under these conditions, the polymer film conforms to the laser-induced stationary temperature profile. Overall, three regions can be distinguished; the bright sharp spot in the center of the micrograph in Figure 2a reflects the size of the focal laser beam, in which high temperatures are reached and a water vapor bubble is formed. In the adjacent inner areas, photothermally induced

deswelling of the polymer film takes place. Because of reflectance changes at the water/polymer/substrate interface, these areas are dark gray, whereas the surrounding outer areas with the swollen polymer film appear lighter. For comparison, Figure 2b shows an intensity profile across the micrograph together with the corresponding temperature profile from calibration experiments. In consistency with a stationary structure, the boundary of the collapsed polymer spot coincides with the radial positions where the LCST of PNiPAAm is reached. Hence, the observed CCD camera

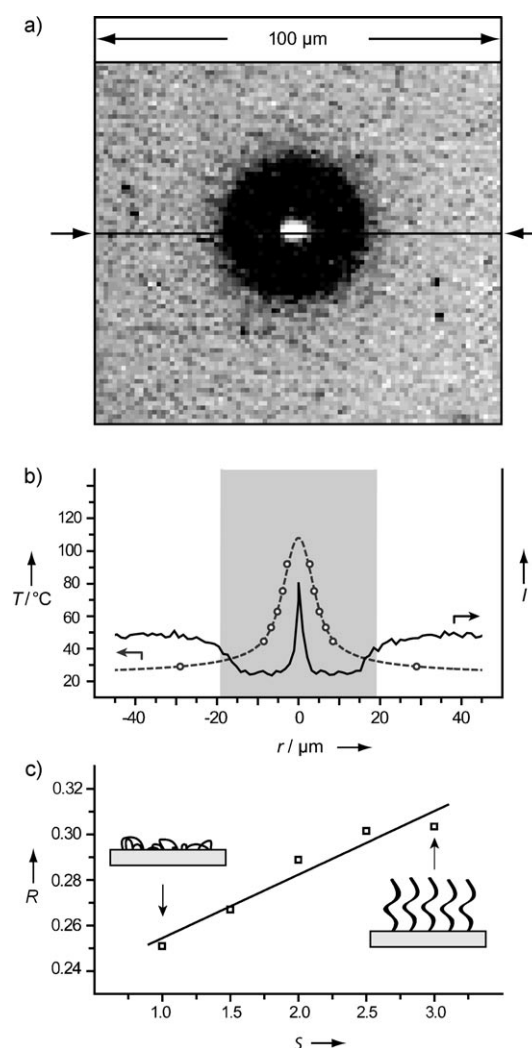


Figure 2. a) Optical micrograph of a PNiPAAm layer upon back surface laser heating taken at the end of a 20 ms laser pulse. The incident laser power is set to 3.1 mW. b) Comparison of an averaged radial profile of intensity I (full line) across the micrograph in (a) and the corresponding radial profile of temperature T (dashed line). The temperature data points (open circles) reflect melting radii as measured in experiments with thin films of long-chain carboxylic acids with distinct melting points between 29°C and 92°C. The analytical solution of the underlying heat conduction equation is fitted with these data. In the gray-shaded area, temperatures above the LCST are reached. c) Results from model calculations of the averaged spectral reflectance R at the water/polymer/Si interface at distinct swelling ratios S between 1 and 3 (square symbols); for comparison a linear fit is shown (full line).

intensity is considered as a relative measure of the swelling ratio S of the polymer brush layer. Complementary optical thin film calculations indeed show that the average reflectance R in the spectral range of the incident light used for illumination, 400–700 nm, follows a weakly pronounced sigmoidal curve in the experimental range between $S=1$ (fully collapsed) and $S=3$ (fully swollen);^[9a] as displayed in Figure 2c. For comparison, a linear fit is shown.

Stroboscopic experiments allow for real-time monitoring of the deswelling and swelling processes (Figure 3). For analysis, the temporal variation of the scaled intensity $I(t)$ at

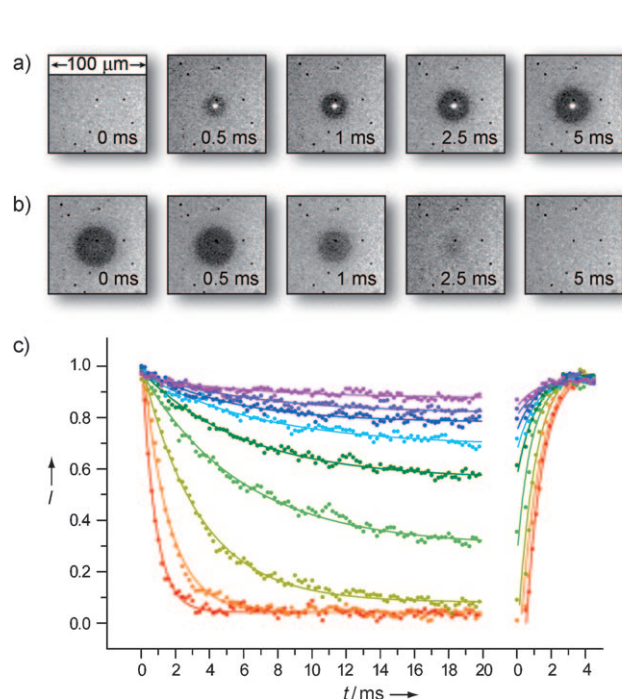


Figure 3. a) Time sequences of micrographs taken during deswelling of a PNiPAAm layer upon back surface laser heating at a laser power of 3.1 mW. b) Corresponding time sequences of micrographs taken during swelling of the polymer layer once the laser is turned off. c) Intensity variations I at distinct radial positions r between 11 μm (red data points, bottom curve) and 30.5 μm (purple data points, top curve) during deswelling (falling curves, left) and swelling (rising curves, right) of a PNiPAAm layer as displayed in (a) and (b). Intensities are scaled between zero (collapsed layer) and one (swollen layer); the lines are fits on the basis of Equation (1) and Equation (2).

distinct radial positions r is considered (Figure 3c). The data closely follow first-order kinetics for deswelling and swelling:

$$I(t) = I_{\infty} \exp(-t/\tau_D), \quad (1)$$

$$I(t) = I_{\infty}(1 - \exp(-t/\tau_S)). \quad (2)$$

Solid lines represent fits on the basis of Equation (1) and Equation (2) leading to response times τ_D and τ_S for deswelling and swelling, respectively. Note that respective heat diffusion times are more than one order of magnitude smaller, that is, upon irradiation, a stationary temperature profile is established on a much shorter time scale.^[7,8a] Hence, these data at distinct radial positions in Figure 3c reflect the

temperature-dependent deswelling kinetics of the polymer film (Figure 4a). In addition, the intensity levels I_{∞} at long irradiation times are proportional to the corresponding stationary swelling ratio S (Figure 4b). Once the laser is switched off, in turn, the heated surface area rapidly cools down.^[7,8a] Thus, irrespective of the radial position, the data in Figure 3c correspond to the swelling kinetics at room temperature and within the error of the measurements all fits give about the same value for the transition rate (Figure 4a) and

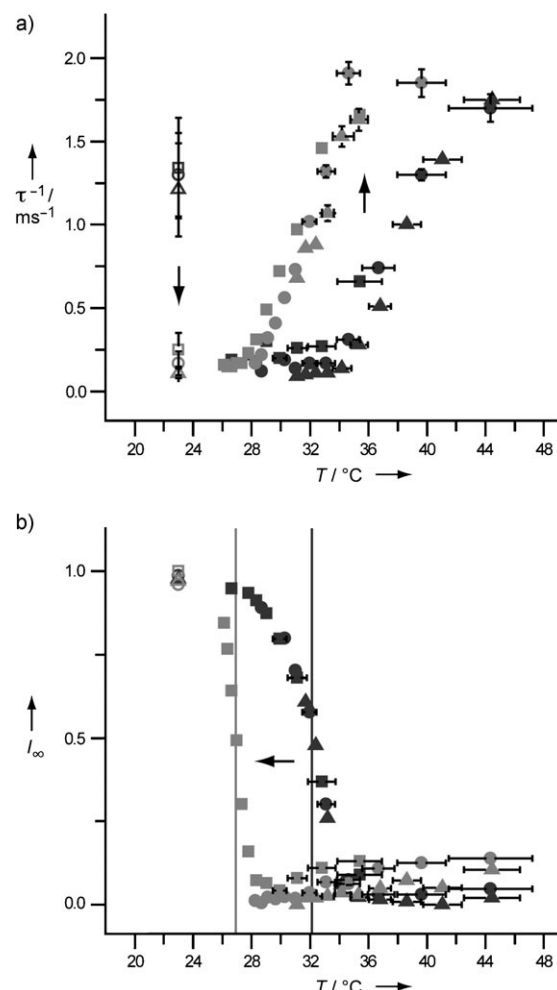


Figure 4. a) Temperature dependence of the switching rates τ^{-1} . b) Temperature dependent variation of the intensity levels I_{∞} at long irradiation times corresponding to the relative stationary swelling ratio S . Dark gray and light gray symbols refer to measurements in water and 0.5 M aqueous solutions of NaCl, respectively. Full and open symbols depict deswelling and swelling data, respectively. Symbols of different shape show data from experiments at a laser power of 2.0 mW (squares), 3.1 mW (circles), and 5.3 mW (triangles). Black arrows indicate changes upon the addition of NaCl. Vertical lines in (b) represent respective positions of the LCST in water and in NaCl solution. Error bars depict statistical uncertainties of the experiments; statistical uncertainties of the switching rate and the intensity at long irradiation times refer to the curve fit errors and the statistical spread of the fit results, respectively, whichever is larger. Statistical uncertainties of the temperature arise because of the limited digital resolution of the micrographs. Error bars that are smaller than the symbol sizes are not shown.

the stationary swelling ratio (Figure 4b).

For comparison, Figure 4 shows results from complementary measurements in a dilute NaCl solution under otherwise identical conditions. These results reveal an asymmetric dependence of the switching processes on the ionic strength, that is, upon addition of NaCl, deswelling rates increase whereas swelling rates become smaller; these findings nicely complement previous thermodynamic studies.^[10] Most notably, however, these data unambiguously show that the measurements are not limited by the thermal equilibration process at the water/substrate interface, but indeed reflect the intrinsic switching kinetics of the polymer brush film. In particular NaCl only marginally alters the thermal properties of water at low concentrations, if at all. Moreover, any change of the thermal properties would not explain the opposing effect on the deswelling and swelling rates.

In conclusion, a novel all-optical micromanipulation/characterization technique for real-time parallel measurements of temperature-dependent kinetic processes at solid/liquid interfaces is presented. The results discussed herein provide unprecedented insight into the complex kinetic processes that rule the switching behavior of ultrathin surface-grafted PNIPAAm brushes when their transition from one to another thermodynamically stable state is triggered by an instant external stimulus. In consistency with what is expected from studies that focus on macroscopic gels, intrinsic response times range from the microsecond to the millisecond time scale, thus demonstrating the prospects of ultrathin surface-grafted polymer films for fabrication of nanosized polymeric actuators and sensors with unmatched responsiveness. Further studies will help to unveil the dependence of the intrinsic switching kinetics of ultrathin thermoresponsive polymer films on their chemical structure/architecture and external parameters. In addition, studies on folding and unfolding of surface-bound protein layers are tempting.

Received: January 7, 2011

Revised: March 8, 2011

Published online: April 14, 2011

Keywords: laser chemistry · polymers · real-time measurements · stimuli-responsive polymers · swelling kinetics

- [1] a) L. Dong, A. K. Agarwal, D. J. Beebe, H. Jiang, *Nature* **2006**, *442*, 551–554; b) D. J. Beebe, J. S. Moore, J. M. Bauer, Q. Yu, R. H. Liu, C. Devadoss, B. H. Jo, *Nature* **2000**, *404*, 588–590; c) L. Dong, H. Jiang, *Soft Matter* **2007**, *3*, 1223–1230; d) M. E. Harmona, M. Tang, C. W. Frank, *Polymer* **2003**, *44*, 4547–4556; e) M. L. Bruening, D. M. Dotzauer, P. Jain, L. Quyang, G. L. Baker, *Langmuir* **2008**, *24*, 7663–7673; f) Q. Yang, N. Adrus, F. Tomicki, M. Ulbricht, *J. Mater. Chem.* **2011**, *21*, 2783–2811; g) L. Ionov, S. Sapra, A. Synytska, A. L. Rogach, M. Stamm, S. Diez, *Adv. Mater.* **2006**, *18*, 1453–1457.
- [2] a) R. C. Advincula, W. J. Brittain, K. C. Caster, J. R  he, *Polymer Brushes: Synthesis Characterization, Applications*, Wiley, Weinheim, **2004**; b) S. Edmondson, V. L. Osborne, W. T. S. Huck, *Chem. Soc. Rev.* **2004**, *33*, 14–22.
- [3] a) W. T. S. Huck, *Mater. Today* **2008**, *11*, 24–32; b) M. A. C. Stuart, W. T. S. Huck, J. Genzer, M. M  ller, C. Ober, M. Stamm, G. B. Sukhorukov, I. Szleifer, V. V. Tsukruk, M. Urban, F. Winnik, S. Zauscher, I. Iuzinov, S. Minko, *Nat. Mater.* **2010**, *9*, 101–113.
- [4] a) G. G. Bumbu, M. Wolkenhauer, G. Kircher, J. S. Gutmann, R. Berger, *Langmuir* **2007**, *23*, 2203–2207; b) E. Spruijt, E. Y. Choi, W. T. S. Huck, *Langmuir* **2008**, *24*, 11253–11260; c) A. J. Parnell, S. J. Martin, R. A. L. Jones, C. Vasilev, C. J. Crook, A. J. Ryan, *Soft Matter* **2009**, *5*, 296–299; d) M. Popa, S. Angeloni, T. B  rgi, J. A. Hubbell, H. Heinzelmann, R. Pugin, *Langmuir* **2010**, *26*, 15356–15365.
- [5] a) T. Tanaka, D. J. Fillmore, *J. Chem. Phys.* **1979**, *70*, 1214–1218; b) T. Tanaka, E. Sato, Y. Hirokawa, S. Hirotsu, J. Peetermans, *Phys. Rev. Lett.* **1985**, *55*, 2455–2458; c) E. Sato Matsuo, T. Tanaka, *J. Chem. Phys.* **1988**, *89*, 1695–1703.
- [6] a) S. H. Gehrke, *Adv. Polym. Sci.* **1993**, *110*, 81–144; b) S. Zhou, C. Wu, *Macromolecules* **1996**, *29*, 4998–5001.
- [7] M. Mathieu, N. Hartmann, *New J. Phys.* **2010**, *12*, 125017.
- [8] a) D. B  uerle, *Laser Processing and Chemistry*, Springer, Berlin, **2000**; b) H.-G. Rubahn, *Laser Applications in Surface Science and Technology*, Wiley, Weinheim, **1999**.
- [9] a) A. Friebe, M. Ulbricht, *Langmuir* **2007**, *23*, 10316–10322; b) M. Mathieu, A. Friebe, S. Franzka, M. Ulbricht, N. Hartmann, *Langmuir* **2009**, *25*, 12393–12398.
- [10] Y. Zhang, S. Furryk, D. E. Bergbreiter, P. S. Cremer, *J. Am. Chem. Soc.* **2005**, *127*, 14505–14510.